Dynamic modeling/simulation of complex power systems using PSS/E

N.H. Abbasy and W.M. Al-Hasawi
College of Technological Studies, Electrical Technology Dept.,, Shuwaikh, P.O. Box 42325, 70654 Kuwait

Planning and operation studies of complex power systems require accurate and reliable modeling of each system component, in addition to a powerful dynamic simulation tool. This paper handles the dynamic modeling and simulation of complex power systems using PSS/E, as being one of the most efficient dynamic simulation tools. The building blocks of the dynamic model of a power system are discussed. Details of modeling Kuwait power network are presented. Dynamic simulations are conducted, where a comparison is made between simulation results of real disturbances and those recorded by actual disturbance recorders (historical data). Based on this comparison, model parameters are tuned-up for more realistic system simulation. Sample contingencies are simulated and system performance is assessed.

تتطلب دراسات التخطيط والتشغيل لنظم القوى الكهربائية المركبة نمذجة دقيقة ومعتمدة لكل مكون من مكونات النظام، بالإضافة إلى وجود أداة محاكاة فعالة. يعالج هذا البحث نمذجة ومحاكاة نظم القوى الكهربائية الديناميكية المركبة باستخدام برنامج PSS/E، وذلك باعتباره واحدا من أكفأ أدوات المحاكاة الديناميكية. يستعرض البحث وحدات التركيب البنائي للنموذج الديناميكي لأي نظام قوى، كما يتم بناء النموذج الديناميكي لنظام القوي الكهربائية بدولة الكويت. يقوم البحث بإجراء المحاكاة الديناميكية على الشبكة الممثلة، حيث يتم عقد المقارنة بين نتائج المحاكاة لاضطرابات حقيقية في النظام والبيانات التاريخية للنظام المسجلة بواسطة مسجلات الاضطرابات. تستخدم تلك المقارنة في ضبط قيم ثوابت النماذج الديناميكية المستخدمة، وذلك من أجل الحصول على نتائج محاكاة أكثر واقعية. كما يتم محاكاة عينات من حالات الطوارئ للنظام وتقييم أداءه. ويختتم البحث باستعراض الخلاصة والاستنتاجات.

Keywords: Dynamic simulation, PSS/E, Model validation, Complex networks

1. Introduction

The requirements for improving the stability of electric power systems and reducing the effect of abnormal system conditions on sensitive customers can be met only by better understanding of the behavior of the system and optimized configuration of the different protection and control systems. This has brought-up the need for improved quality of simulation of normal and abnormal system conditions, which is possible only when using advanced simulation tools based on accurate system models. Confidence in the results from different steady state, dynamic or transient studies is possible when the recordings of power system events or disturbances closely match the results from the simulation of the same event [1]. The accuracy of the different simulations and the assessment of steady state and dynamic security are determined to a great extent by the accuracy of the models.

State-of-the-art power system simulation programs [2-6] are designed to provide comprehensive and accurate simulation of different power system conditions, including power flow, dynamic stability, short circuit analysis, motor start-up, protective relays coordination, and electromagnetic transients. In addition, research efforts have been conducted for modeling specific power system components and/or power systems of special design [7-10]. Using these simulations, planning, operations, protection and control or power quality engineers can analyze the behavior of the system and optimize the performance of different primary or secondary power system equipment. However, the results of the simulations will be accurate and reliable only when the model of the system is correct. The modeling of the system is very challenging because it is continuously changing and includes a huge number of elements.

In this paper, the building blocks of the dynamic model of a power system are

discussed. Details of modeling Kuwait power network are presented. Dynamic simulations are conducted, where a comparison is made between simulation results of real disturbances and those recorded by actual disturbance recorders (Historical data). Based on this comparison, model parameters are tuned-up for more realistic system simulation. Sample contingencies are simulated and system performance is assessed.

2. Model preparation

The dynamic simulation of a power system can be accomplished via two major modules; Load Flow (LF) and Dynamic Simulation (DS) modules. The earliest step in PSS/E simulation of a power system is the preparation of the Load Flow case. The output file of this stage is referred to as the Load Flow Unconverted Case (LFUC). In the DS module, a dynamic raw data file is prepared. This file includes data relevant to the dynamic models of the system components. Thereafter, both network LF data and dynamic data are combined into one file, called the snapshot file. Then, the simulation (run) stage follows immediately. Different system components are modeled using built-n dynamic models. The selection among the available models is justified according to the manufacturer data provided with the plant installation. For example, generators are modeled as solid rotor generators at the sub-transient level. Exciters are modeled as a potential source controlled rectifier, where excitation power is supplied through a transformer from the generator terminals (or the unit's auxiliary bus) and is regulated by a controlled rectifier.

As per load modeling, there are four distinct methods for load modeling based PSS/E; namely, constant MVA, modeling, constant current modeling, constant admittance modeling, and composite modeling.

In constant MVA modeling, the load boundary condition is a specification of load real and/or reactive power consumption, as given by eqs. (1) and (2) (for bus # k):

$$Real(v_k i_k^{*}) = -P_k \quad . \tag{1}$$

$$Imag(v_k i_k^{*}) = -Q_k \quad . \tag{2}$$

In constant current modeling, loads may be specified as a given active or reactive component of current. These models make load dependent on frequency in accordance with:

$$\frac{Real(v_k\, i_k^{*})}{|v_k|} = -I_{pk}, \tag{3}$$

$$\frac{Imag(v_k\, i_k{*})}{|v_k|} = -I_{qk} \, . \tag{4}$$

In constant admittance models, load may be specified by given real and reactive parts of shunt admittance such that:

$$\frac{i_k}{v_k} = G_k + j B_k \, . \tag{5}$$

As per the composite load modeling, all PSS/E network solutions allow the load at each bus to be a composite of arbitrary amounts of load with each of the above three characteristics. The composite characteristic becomes the boundary condition used in iterative power flow solutions. A fraction of the constant MVA load at each bus is transferred to each of the other two load characteristics, according to the following equation:

$$\begin{aligned} S_I &= S_i + \frac{aS_p}{V}, \\ S_Y &= S_y + \frac{bS_p}{V^2}, \\ S_P &= S_p \times (1 - a - b) \, , \end{aligned} \tag{6}$$

where S_p, S_i, S_y are the original constant MVA, constant current and constant shunt admittance load, respectively, and S_P, S_I, S_Y are the corresponding final nominal values. Constants a, b are arbitrary chosen load transfer fractions (where $a + b < 1$), and V is the magnitude of bus voltage when load conversion is made. In case of Kuwait system, loads are arbitrary composed according to the following ratios: 80, 0 for active power and 40,

20 for the reactive power. This means that active power load is modeled with 80%, 0% and 20% as constant current, constant conductance and constant MVA, respectively. Similarly, reactive power load is modeled with 40%, 20% and 40% as constant current, constant conductance (admittance) and constant MVA, respectively.

One more relevant aspect is the frequency dependence of loads. The LDFR family of models provided by PSS/E makes the constant current and MVA components of all loads, to which the model is applied, dependent on bus frequency. These models make load dependent on frequency in accordance with:

$$P = P_o\left((\frac{\omega}{\omega_o})^m\right), \quad Q = Q_o\left((\frac{\omega}{\omega_o})^n\right)$$
$$I_p = I_{po}\left((\frac{\omega}{\omega_o})^r\right), \quad I_q = I_{qo}\left((\frac{\omega}{\omega_o})^s\right), \qquad (7)$$

where constants *m, n, r,* and s are selected by the user and stored in as CONs. These indices are not necessarily integers, and may be zero if the corresponding load components are independent of frequency. In case of Kuwait system, loads are categorized into 4 categories; industrial, auxiliary, distillation and residential. Constants *m, n, r*, and s are selected for each category. Typical values are: m = 2, n = 0, r = 2, s = 0. The current setting for these load models is as follows: for residential/industrial load: m = 1.5, n = 0, r = 1.5, s = 0; for plant auxiliary /distiller load: m =2, n = 0, r = 2, s = 0. Obviously, there is no rule of thumb for assigning these constants. However, these constants can be fine-tuned through a comprehensive comparison between simulation results and actual results obtained by recorders.

3. Simulations and assessment

Kuwait network is used as a case study to validate and assess the dynamic models presented in this paper. In this system, underfrequency relays are set such that they automatically disconnect predetermined load centers according to the level of the declined frequency, in case of generation deficiency. This underfrequency load-shedding scheme adopts an overall number of 5 stages, where relays automatically trip at 49, 48.7, 48.4, 48.2, and 48 Hz for stages 1 through 5 respectively

Table 1 presents the details of abnormal incidents encountered the system during 2002-2003 period. Figs. 1 through 4 show the simulated frequency response of the system for cases 1 through 4 of table 1, whereas the actual recorded tracings for case 1 is provided in fig. 5. Actual frequency tracings of the remaining cases were omitted for limited space.

3.1. Model validation

In order to validate the models used in this system, 4 different abnormal incidents were recorded and simulated. It is noticed that among these cases, case #1 is the only one that required underfrequency load shedding. In order to simulate these disturbances using PSS/E, the dynamic simulation was run for one half-cycle (0.01 s based-50 Hz) prior to the disturbance. This brought up the simulation up to t =0 (the instant of disturbance). At that instant the disturbance was applied by dropping specific units as listed in table 1. Thereafter, simulation was advanced for two seconds right after the disturbance in order to determine the time instant at which system frequency would hit the first stage load shedding frequency threshold (49.0 Hz). Once this instant was determined, the simulation was repeated where the first stage load shedding was activated at its predetermined time instant (after accounting for an additional 100 ms as a time delay for relay operation). Then, the whole procedure was repeated to check for the necessity of activating the 2nd, 3rd,..., stages, respectively. In this simulation, it was found that 3 load-shedding stages were necessary to restore the system frequency, with a total reduction in system loads of 714 MW. This result totally agreed with the actual system behavior described in table 1, case # 1. The close inspection of figs. 1 to 5 show that both responses yielded almost identical values for the minimum frequency. (48.34 Hz). The time elapsed for the system to reach this minimum frequency was also identical (2.5 s). Moreover,

Table1
Details of the abnormal incidents during 2002-2003

Day/date	Case # 1 Monday 23-12-2002	Case # 2 Thursday 27-2-2003	Case # 3 Monday 10-2-2003	Case # 4 Monday 03-03-2003
Case Number	Case # 1	Case # 2	Case # 3	Case # 4
Location	DWPS	DWPS	ZSPS	ZSPS
Time	13:30	10:57	10:00	17:37
System load (MW)	2980	2680	2630	3020
Plants on bar (MW)	3150	4550	4715	4640
ISR (MW)	490	675	725	675
Contingency	All circuits, which are connected to the 300 kV bus at DWPS, tripped, causing an outage of 900 MW.	Unit 8 tripped due to tripping of it boiler on "drum level three low" indication, while it was carrying 160 MW.	Unit 5 tripped due to tripping of its boiler on "function group control power supply failure" indication, while it was carrying 120 MW.	Unit 2 tripped due to tripping of its boiler on "boiler control supply failure" indication, while it was carrying 170 MW.
Number of units in service	SB (3); ZS (5); DE (4); SS (4); DW (5)	SB (3); ZS (5); DW (4); DE (4); SS (3)	SB (4); ZS (4); DW (5); DE (4); SS (2)	SB(4); ZS(4); DW(5); DE(4); SS(3)
Plant generation (MW)	SB (504); ZS (860); DE (345); SS (368); DW (900)	SB (480); ZS (800); DW (800); DE (350); SS (250)	SB (650); ZS (650); DW (800); DE (350); SS (180)	SB (600); ZS(850); DW(850); DE(450); SS(270)
Frequency (Hz)	Dropped from 50.02 to 48.32	Dropped from 50.02 to 49.85	Dropped from 50.01 to 49.85	Dropped from 50.01 to 49.79
Plant pick-up (MW)	SB (15); ZS (145); DE (55); SS (55) +3 stages of the automated under frequency scheme operated causing a loss of supply of total 714 MW.	SB (30); ZS (60); DW (40); DE (20); SS (10). No load shed.	SB (30); ZS (30); DW (40); DE (15); SS (5). No load shed.	SB (50); ZS (50); DW (45); DE (15); SS (10). No load shed.

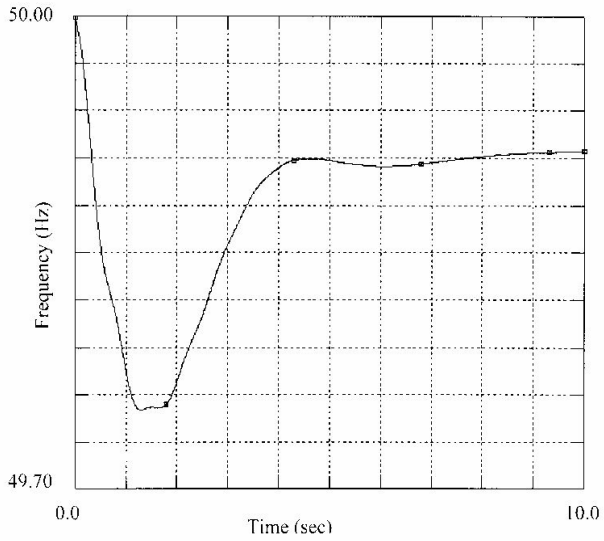

Fig. 1. System frequency response for case # 1.

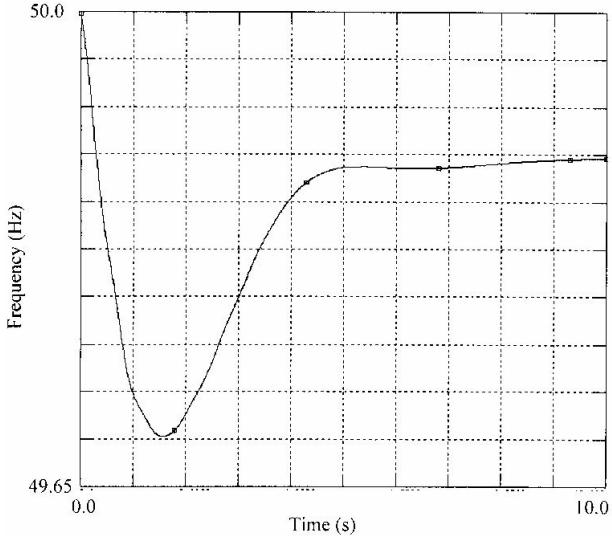

Fig. 2. System frequency response for case # 2.

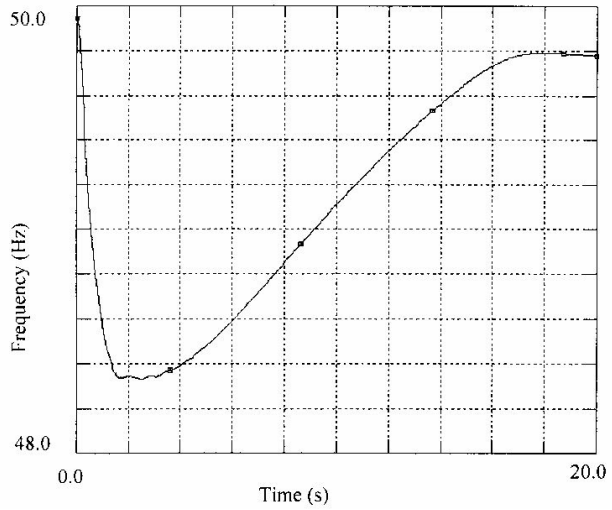

Fig. 3. System frequency response for case # 3.

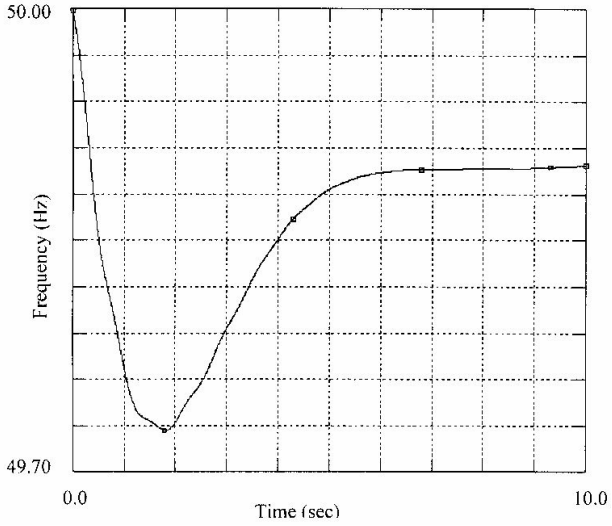

Fig. 4. System frequency response for case # 4.

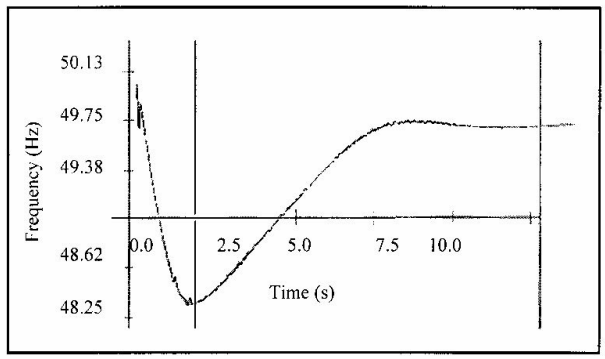

Fig. 5. System tracing of disturbance recorder for case #1.

the new stabilized (steady state) frequency was fairly close (about 49.65 Hz) in both responses, giving the same steady state frequency error (0.35 Hz). However, a substantial deviation is observed in the restoration time of both responses. The actual system response required about 6 s to re-stabilize, while the simulation response required about 15 s to re-stabilize. From a practical prospective, this discrepancy is of less importance; as frequency restoration time is not a planning parameter in any operational scheme, e.g., load shedding. On the other hand, the result is optimistic by itself, since the actual system restoration is faster than what the simulation gives. In cases 2, 3 and 4, where load shedding was not required, the simulation was advanced for adequate period of time (e.g. 10 s) until frequency re-stabilized.

Table 2 shows a comparison between the actual recorded results with those obtained from simulations. This comparison is limited to restoration time, value of minimum frequency, the time required to reach the minimum frequency, the initial rate of frequency decline, and finally the steady state frequency. The % deviation, defined as [(simulated response - recorded response) / recorded response]*100, is also computed and shown in the same table.

From table 2, the following observations can be made:

1. The actually recorded restoration times are much longer than the simulated times.
2. The actually recorded minimum frequency reached in each case is slightly higher than the simulated values (except case #1).
3. The actually recorded times to reach minimum frequency are sometimes higher than the simulated times and sometimes lower.
4. The actually recorded rate of frequency decay is less than the corresponding simulated values.
5. The actually recorded steady state frequency is higher than the corresponding simulated values.
6. In the actual recorded data, a slight "overshoot" for the frequency is observed before it settles at its steady state value. In case of simulated data, the frequency rises

smoothly to the new equilibrium state without overshooting.

In view of the above observations, it can be generally concluded that the simulation results are more accurate (closer to the actual recorded results) in terms of frequency (whether minimum or steady state) and less accurate in terms of system restoration time, initial rate of frequency decline and time to reach minimum frequency. Nevertheless, the deviation in simulation results is always in the "pessimistic" side, in the sense that worst system response is obtained via simulation. This latter observation implies that the simulation results are always in the safe side in spite of not being highly accurate.

3.2. Tuning of model parameters

In view of the observation made at the end of the previous section, an attempt was made to narrowing the gap between the two responses, during the restoration period. The difference of restoration time may be attributed to different factors. The complexity and diversity of loads existing in the system, the uncertainty of system model parameters, and the inaccuracy of actual system recordings may represent some of these factors. However, there are actually 4 load categories in the present system. These are: residential, industrial, distillation and plant auxiliary. Referring back to the LDFR family of models given by eq. (6), three attempts of frequency dependent load modeling were made, with the following parameters:

1. $m = 1.5$, $n = 0$, $r = 1.5$ and $s = 0$
2. $m = 2$, $n = 0$, $r = 2$ and $s = 0$
3. $m = 3$, $n = 0$, $r = 3$ and $s = 0$

Fig. 6 shows the frequency behavior during the present disturbance for these three models. Compared with the actual recorded frequency during this fault, it is obvious that the third load model mimic the actual response more accurately. This proved the fact that better system performance can be achieved through tuning some of model parameters. This era requires extensive trials and revaluation of the models adopted.

Table 2
Comparison between results of actual and simulated disturbances

Case #		Case # 1 23-12-2003	Case # 2 27-2-2003	Case # 3 10-2-2003	Case # 4 3-3-2003
Restoration time (s)	Recorded	8.28	3.76 s	4.10 s	3.77 s
	Simulated	16.32	7 s	4.3 s	5.02 s
	% Deviation	97%	86.17021	69.65551	33.1565
Min. freq. (Hz)	Recorded	48.238	49.85 Hz	49.85 Hz	49.79 Hz
	Simulated	48.32	49.726 Hz	49.75 Hz	49.691 Hz
	% Deviation	-0.016	-0.24875	-0.2006	-0.19884
Time to reach Min. freq. (s)	Recorded	1.7	1.654 s	1.91 s	1.34 s
	Simulated	2.51	1.78 s	1.43 s	1.522 s
	% Deviation	47.64	7.617896	-25.1309	13.58209
Initial rate of freq. decay (Hz/s)	Recorded	1.728	0.0906 Hz/s	0.0785 Hz	0.162 Hz
	Simulated	2.14 Hz	0.1539 Hz	0.175 Hz	0.203 Hz
	% Deviation	-17.07	69.86755	122.9299	25.30864
Steady state frequency (Hz)	Recorded	49.65	49.95 Hz	49.96 Hz	49.98 Hz
	Simulated	49.61	49.899 Hz	49.914 Hz	49.892 Hz
	% Deviation	-0.08	-0.1021	-0.09207	-0.17607

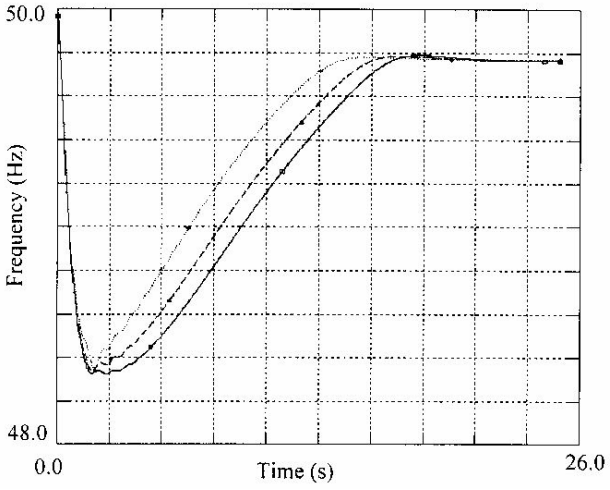

Fig. 6. Frequency responses for three LDFR models.

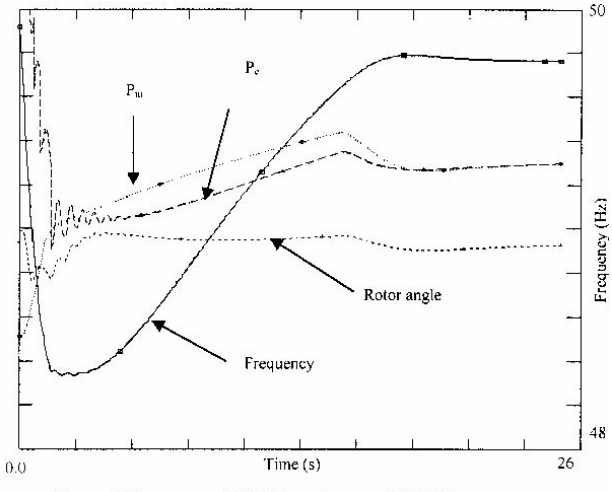

Fig. 7. Response of ZSPS to outage of DWPS scale: P_e P_m: 150:220 MW, rotor angle:-10°:15°.

3.3. Performance assessment

The response of system generating plants to the outage shown in case #1, table 2 was monitored using activity "CHAN". Fig. 7 summarizes the response of ZSPS to that outage. This response includes the total electrical power, total mechanical power, machine rotor angle, and system frequency measured at that plant. Similar plots for the remaining plants were obtained but not shown. Fig. 8 shows the sum of mechanical power of all system units for that outage.

To check unit's response to generation outages, a different simulation was performed. Fig. 9 shows DWPS unit response at a trip of one unit at ZSPS. The system frequency, the mechanical and electrical power, as well as the machine rotor angle of that particular unit were monitored and plotted in that figure. The mechanical power curve shows how the instantaneous spinning reserve (ISR) builds up to share in the alleviation of the deficit of generation due to the outage. This ISR response started fairly fast (within 5 s), then its rate slowed down thereafter. Also both electrical and mechanical power of that unit coincided when the system frequency re-stabilized at 49.6 Hz, leaving a steady state frequency error of 0.4 Hz. Obviously, this trip did not require any load shedding as the decay of system frequency halted at 49.75 Hz before the 1st stage frequency level of system automatic load shedding scheme. Finally, a third simulation was conducted to assess the system response at line faults. The line connecting JAHRW and SLYBW was faulted at t =2 s. This fault sustained for about 5 s, where the fault was cleared at t = 7 s. Fig. 10 shows the system frequency and voltage at SRRD for this contingency. The simulation shows that it took about 30 s for the frequency to re-stabilize, where the system frequency fluctuated between 53.75 and 48.85 Hz, whereas the voltage at SRRD fluctuated between 85 and 408 kV. The voltage monitored at SRRD stabilized at about 5.5% above normal. This result would have impact on insulation coordination of the system to withstand such switching over voltages.

4. Conclusions

This paper presented a procedure for dynamic modeling and simulation of complex power systems using PSS/E. Dynamic simulations of real disturbances were conducted and results were compared with those obtained by system disturbance recorders. Based on this comparison, the dynamic model parameters of system loads were fine-tuned for more realistic dynamic simulation. The system dynamic behavior in case of unit outage, plant outage, and line faults was assessed. Further studies related to the switching impact on system over

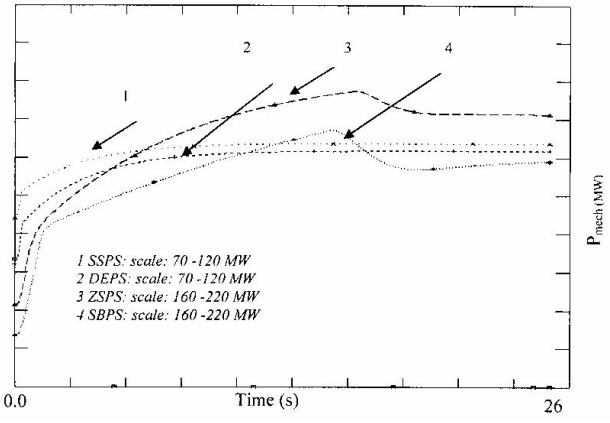

Fig. 8. Unit's mechanical power for outage of DWPS.

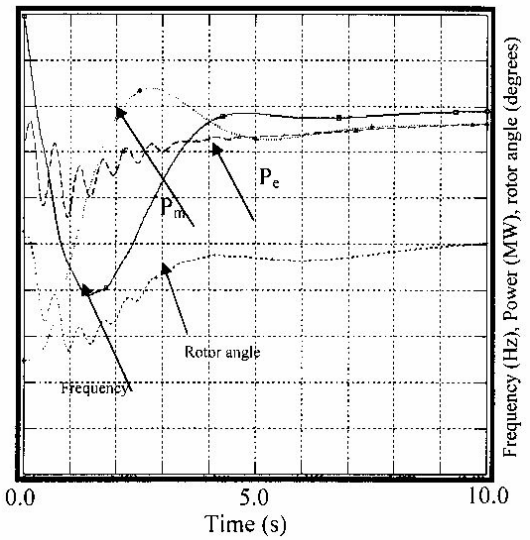

Fig. 9. DWPS unit for trip at ZSPS scale: frequency: 49.6 50 Hz, P_e, P_m 175:195 MW, Rrotor angle 0°:2.5°.

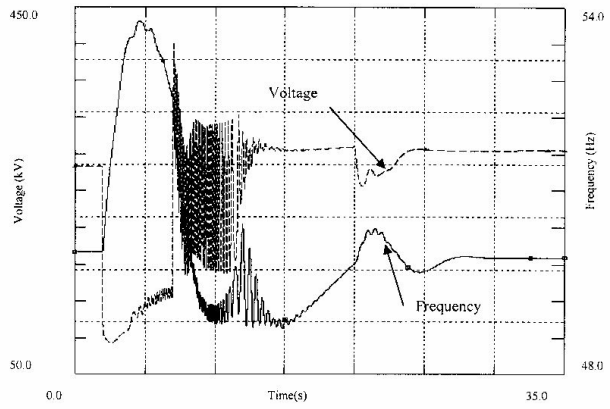

Fig. 10. System frequency and bus voltage at SRRD for line fault.

voltage and the proper allocation of dynamic system reserve can be conducted by following the simulation procedure shown in this paper. It is believed that this paper would generally assist students, researchers, and electrical utility engineers in modeling and simulation of complex power systems.

Acknowledgement

The authors are grateful to the staff of The National Control Center, Kuwait, for providing the data and relevant information of Kuwait power network.

References

[1] Alexander Apostolov, "Verification of System Models for Steady-State and Dynamic Security Assessment", Proceedings of the 37th Hawaii International Conference on System Sciences (2004).

[2] GE Power Systems Analysis Software, General Electric International Inc.

[3] Simsen: A Modular Software Package for the Analysis of Power Networks and Electrical Machines, ICEM 94.

[4] Matlab the Language of Technical Computing, version 6.1.0.450, Release 12.1, 18 (2001).

[5] ETAP Power Station, 3.0, Operation Technology, Inc. (2001).

[6] ATP-EMTP, Canam EMTP User Group.

[7] P. Sakis Meliopoulos, George J. Cokkinides, and Robert Lasseter, "A Multiphase Power Flow Model for μGrid Analysis", Proceedings of the 36th Hawaii International Conference on System Sciences (HICSS'03), 0-7695-1874-5 (2003).

[8] W.J. Peet, Babcock and Wilcox, "Development and Application of a Dynamic Simulation Model for a Drum Type Boiler with Turbine Bypass System," International Power Engineering Conference, March, Singapore (1995).

[9] Debabrata Chattopadhyay, and Ross Baldick," Unit Commitment with Probabilistic Reserve," Proc. of IEEE PES Winter Meeting, New York, USA.

[10] F.W. Koch, I. Erlich, and F. Shewarega," Dynamic Simulation of Large Wind Farms Integrated In A Multi Machine Network," IEEE PES 2003 General Meeting, July 13-17, Toronto, Canada (2003).

Received May 12, 2004
Accepted September 13, 2004